Brief Reports

Brief Reports are accounts of completed research which, while meeting the usual **Physical Review** *standards of scientific quality, do not warrant regular articles. A Brief Report may be no longer than four printed pages and must be accompanied by an abstract. The same publication schedule as for regular articles is followed, and page proofs are sent to authors.*

X-ray thermal-diffuse-scattering study of soft modes in paraelectric $BaTiO_3$

Naohisa Takesue
Department of Materials Science and Engineering, University of Illinois at Urbana-Champaign, Urbana, Illinois 61801

Mario Maglione
Laboratoire de Physique, Universite de Bourgogne, Batiment Mirande, B. P. 138, 21004 Dijon Cedex, France

Haydn Chen
Department of Materials Science and Engineering, University of Illinois at Urbana-Champaign, Urbana, Illinois 61801
(Received 12 September 1994)

Anomalous x-ray thermal diffuse scattering (TDS) from the paraelectric $BaTiO_3$ has been measured as a function of temperature using synchrotron radiation. Sheets of intensities that were previously reported have been confirmed. The origin of the observed TDS intensities is attributed to the soft on-(100) TA modes and overdamped $[010]_{TO}$ mode for reduced wave vector $q > 0.25$ and < 0.25, respectively. In agreement with the previous neutron inelastic scattering experiment, our results support the notion of the one-dimensionally correlated optic motion of atoms.

The anomalous diffuse x-ray scattering in the form of two-dimensional sheets on $\{100\}$ planes of the reciprocal-lattice space has been reported in $KNbO_3$ (Refs. 1, 2, and 4) and $BaTiO_3$ (Refs. 1–3), indicating the presence of one-dimensional (1D) correlation in real space. There have been two theoretical models proposed to explain the origin of the diffuse sheets from those perovskite ferroelectrics; one is the Hüller's model[5,6] based upon the soft-optic dipole interaction and the other is proposed by Comes, Lambert, and Guinier,[1,2] the eight-site static model of the order-disorder type. Both models appear to have some success in explaining experimental observations.

Associated with the Lyddane-Sachs-Teller relation derived based upon the lattice dynamics of the ferroelectric phase transformation,[7] neutron inelastic-scattering experiments[8,9] have been performed in $BaTiO_3$ to investigate the actual vibrational modes in the paraelectric phase at temperature $T > T_c \approx 130\,^{\circ}C$. It was clearly shown that the $[100]_{TO}$ mode is overdamped[8–11] with a significant temperature dependence[8] of the scattering intensity at small q around the zero neutron energy loss. From the experimental data,[5,6,9] it was found that the energy for any **q** vector with the [001] polarization on the (001) plane has low values all over the zone, while those with the same polarization out on the (011) rapidly increase with increasing magnitude of **q**. As predicted by Hüller,[5,6] owing to this anisotropy of the phonon-dispersion relationship, diffuse intensity sheets on the $\{100\}$ planes would exist. Results of the neutron inelastic-scattering experiments appeared to support Hüller's model.

On the contrary, in the model of Comes, Lambert, and Guinier,[1,2] they suggested that the crystal potential-energy surface has a maximum for the cubic perovskite structure and eight (degenerate) minima for the $\langle 111 \rangle$ displacements of the body-centered Ti or Nb ion. In this picture, the relevant dynamics consist mainly of hopping among these eight minima (relaxation mode). They thus predicted from the 2D diffuse intensity distribution that the static chain structure might exist if the off-centered Ti (Nb) ions are linearly correlated.

Studies in the past decade for the ferroelectric phase transformation in $BaTiO_3$ (Refs. 12–16) have had varied opinions; some suggested the possible existence of the soft mode, others favored the static chain model, or even the coexistence of both. The electron-paramagnetic-resonance experiment[12] has detected that Mn^{4+} (substitutional of Ti^{4+}) spins are reoriented along the $\langle 111 \rangle$ under the magnetic resonant condition. From the concept that the magnetic and electric ordering may occur at the same temperature,[17] this spin reorientation may manifest a feature of the hopping mode of the Ti ions. However, the resonance has not been found for the other three higher-temperature phases. This study does not prove the existence of the relaxational mode.

The hyper-Raman-scattering experiment has been done for cubic $BaTiO_3$.[13] Analysis has shown that the imagi-

0163-1829/95/51(10)/6696(4)/$06.00

nary part $\varepsilon''(\Omega)$ of the dielectric function can be adequately explained by a classical single oscillator dispersion formula, giving high damping, consistent with the previous studies,[8-11] while Debye relaxator model fails in reproducing the corresponding $\varepsilon''(\Omega)$ profile. The result verifies the existence of the overdamped mode.

Two Raman-scattering experiments[14,15] have revealed the coexistence of both the soft mode and the relaxational mode. The earlier experiment[14] has shown that line profiles corresponding to the overdamped mode and the central peak in the tetragonal phase region were found on the frequency spectra in particular scattering geometries, E and A symmetries, respectively. The more recent measurement[15] has confirmed that both the modes exist over the temperature range of the cubic and tetragonal phases for the soft E phonon, showing superpositioned Raman line profile from the damped mode and central peak. In those cases, it was observed that the scattering intensity from the relaxational mode becomes significantly higher than that from the oscillator mode in the cubic phase region, suggesting that the relaxation totally dominates the cubic-tetragonal transition. The results from the cubic phase may contradict with the Hüller's model, whereas the coexisting overdamped and relaxational mode in the tetragonal phase region can both explain the 2D sheets.

The linearized-augmented-plane-wave method[16] has been employed to compute phonon frequencies and eigenvectors for three optic F_{1u} modes, and has deduced a possibility of co-occurrence of both the modes. Potential surface showed that existing energy wells for the soft-mode distortion (Ti) are deeper for rhombohedral $\langle 111 \rangle$ displacements than tetragonal $\langle 001 \rangle$ displacements, but they were relatively shallow and comparable to the transition temperature. Including a tetragonal c/a ratio, the energy calculation indicated that the tetragonal strain increasing the Ti-O distance significantly stabilizes the tetragonal phase, suggesting the Ti ions spend a considerably long time in the $\langle 001 \rangle$ well, rather than only hopping among the $\langle 111 \rangle$ well. The phase transition is thus thought to be a complicated coupling of a soft mode, order-disorder hopping, and lattice strain.

Thus, we have employed *in situ* x-ray diffuse scattering technique using synchrotron radiation to obtain high quality thermal-diffuse-scattering (TDS) data from a $BaTiO_3$ single crystal in its cubic phase. The objectives of the work are twofold: (1) to reproduce the 2D TDS intensities as previously reported, and (2) to investigate the temperature dependence of the TDS intensities.

We used a poled single crystal of $BaTiO_3$ with the surface normal near $[001]_{cubic}$. The TDS measurements were carried out at NSLS, Brookhaven National Lab. A wavelength of 1.1808 Å was used. Experiments were performed at 200, 150, and 135 °C ($T_c = 132.5$ and 129 °C on heating and cooling).

Diffuse intensity contour maps around the 400 reflection on a (100) plane at 200, 150, and 135 °C are shown in Figs. 1(a), 1(b), and 1(c). Cross-sectional scans through the plane along the [100] direction for several k values at $l = 0$ (hkl are Miller indices), and at 200 °C, are illustrated in Fig. 2. The intensity profile along h shows a sharp peak at $h = 3.95$ for each fixed k. Figures 1 and 2

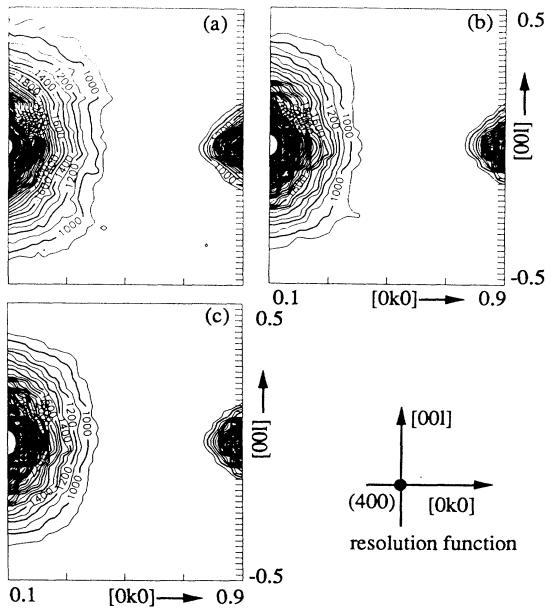

FIG. 1. Equi-intensity contour maps of x-ray diffuse scattering intensities on the (100) plane near the 400 reflection at (a) 200, (b) 150, and (c) 135 °C. An approximate resolution function at the 400 reflection is indicated by a round-shaped mark in the lower right corner.

clearly show that the observed diffuse intensity distribution is two dimensional. To our best knowledge, the present observation represents the most convincing results regarding the presence of diffuse intensity sheets in $BaTiO_3$.

Several noticeable features are found in each of Fig. 1. First, TDS intensities adjacent to the 410 reflection in the next Brillouin zone are considerably weaker than those near the 400 reflection. Secondly, there is a circular-shaped intensity ring around the 400 reflection at all three temperatures for $|\mathbf{q}| > 0.25$ (in terms of reciprocal-lattice units). Thirdly, for $|\mathbf{q}| < 0.25$, diffuse intensities increase steeply toward the 400 location and are elongated along the [010] and [001] direction. These features will be explained based upon the TDS theory[3,18] and

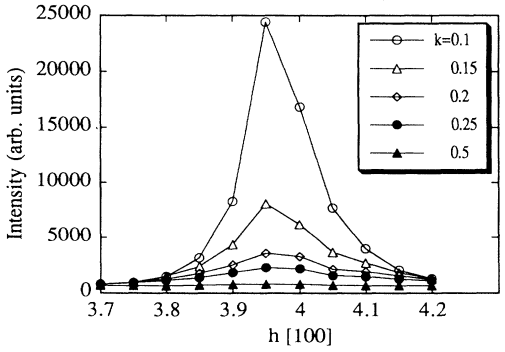

FIG. 2. Intensity profiles of the cross sectional scans through the diffuse scattering plane of Fig. 1(a) along the [100] direction for $k = 0.1$, 0.15, 0.2, 0.25, and 0.5 at $l = 0$ ($T = 200$ °C).

compared with the previous results of the neutron inelastic-scattering study[8,9] as below.

There is almost no measurable intensity at $|\mathbf{q}|>0.25$ from the 410 reflection. Only the steep portion of the TDS intensity is recognized at $|\mathbf{q}|<0.25$. This difference in the strength of the TDS between portions of the 400 and 410 zones is related to the difference in their respective static crystal structure factors.[3] On top of that, TDS intensities are known to decrease when the diffraction vector **S** moves away from the 400 center because of the effect of a geometrical extinction factor as expressed by the direction cosine of an angle determined by a scalar product of **S** and phonon polarization e_{qj}.[18]

For $BaTiO_3$ the static crystal structure factors are expressed as $F(400)=f_{Ba}+f_{Ti}+3f_O$ and $F(410)=f_{Ba}-f_{Ti}-f_O$, where f_{Ba}, f_{Ti}, and f_O are atomic scattering factors of corresponding elements. We see that the structure factor of the 400 reflection is larger than that of 410. As a result, the TDS intensity is expected to be weaker near the 410 peak.

The static crystal structure factor is directly related to the thermal diffuse intensity due to the acoustic mode.[3,18] From the above discussion it was seen that TDS intensities at $|\mathbf{q}|>0.25$ are strongly related to the static structure factor. As a result, it can be thought that the TA modes with **q** in the lowest-energy branch lying on the (100) plane [on-(100) TA modes] contribute most significantly to the TDS intensities. Since there is no appreciable temperature dependence of the phonon frequency, for example for the $[100]_{TA}$ based upon the conclusions reached by the inelastic neutron-scattering results,[8,9] it is thus expected that TDS intensities from the TA mode should be proportional to temperature by way of the Debye-Waller factor effect multiplied by absolute temperature,[18] which usually indicates a negative temperature dependence in the paraelectric region.[19] In fact, the overall TDS intensities shown in Fig. 1 appear to decrease with decreasing temperature.

Noticeably, distribution of the TDS intensities from the low-energy modes around the 400 reflection for any on-(100) TA mode with $|\mathbf{q}|>0.25$ is a circular shaped ring as seen in Fig. 1. The intensities in this part are almost the same at constant $|\mathbf{q}|$ along any on-(100) direction. Since the TDS intensity is basically proportional to $1/\omega_{qj}^2$ (ω_{qj} is a phonon frequency),[18] those circular contour lines represent the equivalent phonon-frequency dispersions of any on-(100) TA mode. From the fact that the significant TDS distribution was observed only on the (100) plane, it is deduced that the dispersion curve of any other mode off the (100) [i.e., off-(100) TA mode] increases rapidly with $|\mathbf{q}|$, showing highly anisotropic behavior.

Line scans along the [001] direction of Fig. 1(a) reveal another feature for the on-(100) TA modes as shown in Fig. 3 for several k values. In this figure, q is defined as $|\mathbf{q}|=(k^2+l^2)^{1/2}$. We find that the TDS distribution is nearly flat at $|\mathbf{q}|>0.25$ because of the circular intensity pattern. In contrast TDS intensities for $|\mathbf{q}|<0.25$ show sharp peaks and appear to have a different temperature dependence. A noncircular TDS pattern can be seen in Fig. 1 where intensities are elongated along the [010] and

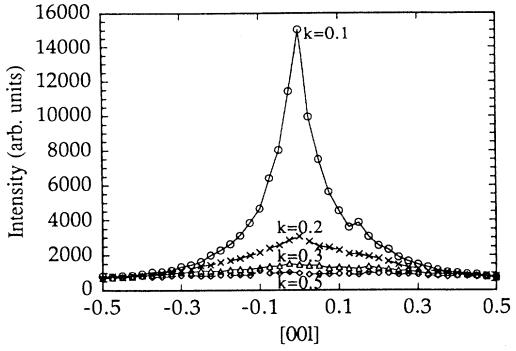

FIG. 3. Intensity profiles of line scans along the [001] direction for $k=0.1$, 0.2, 0.3, and 0.5 at $h=4.0$ on the (100) plane taken from Fig. 1(a) at 200 °C. For $k>0.2$ TDS distribution is very flat. On the other hand, it becomes steep for $k<0.2$. The intensity peaks at $l=0$ for $k=0.1$ and 0.2.

[001] directions corresponding to the strong TDS contribution from the transverse [010] and [001] modes, respectively. In the previous inelastic neutron-scattering experiment,[8,9] a similar intensity distribution was found which is attributed to the highly damped $[100]_{TO}$ and $[010]_{TO}$ mode with the [001] polarization. This overdamped TO mode should manifest itself in the x-ray TDS intensities as well. The TDS intensities due to the overdamped TO modes is not expected to be as clear as those of the previous neutron data because the low-energy on-(100) TA modes also contributes to the total diffuse x-ray-scattering intensities. Nevertheless, a similar pattern has been detected with x rays in the current study, meaning the intensity ridges from the overdamped $[010]_{TO}$ and $[001]_{TO}$. Sharp ridges of TDS intensities adjacent to the 400 reflection are clearly seen in Fig. 3. For $k=0.1$ and 0.2 peaks are located at $l=0$, whereas a broader bump is observed for $k\geq 0.25$.

The temperature dependence of the TDS intensities is presented in a different form in Fig. 4 where intensities along the [0k0] at $l=0$ are displayed. One may compare the neutron results with the current x-ray results on a qualitative basis. The neutron-scattering intensities from the overdamped $[010]_{TO}$ at $\mathbf{Q}=(2.0,0.076,0.0)$, which corresponds to $|\mathbf{q}|=0.076$ along the [010] direction, was found to increase with decreasing temperature from 160 to 137 °C.[8] The x-ray TDS intensities behave very much in a similar way when temperature is decreased from 200 to 135 °C for $k<0.25$ near the 400 reflection as shown in Fig. 4(a). The magnitude of the intensity drop may not be as much for the x-ray data as those for neutrons because of the contribution from the TA mode in the former. TDS contribution from the TA mode will generally give rise to a higher background level and is expected to decrease in proportion to the temperature along with the Debye-Waller factor effect.[18] In spite of these complications, the temperature-dependent behavior as reported in the neutron study is reproduced in the current x-ray TDS study.

TDS intensities from the overdamped $[010]_{TO}$ mode for $k>0.75$ near the 410 reflection [Fig. 4(b)] show a positive temperature dependence, opposite to the behavior for

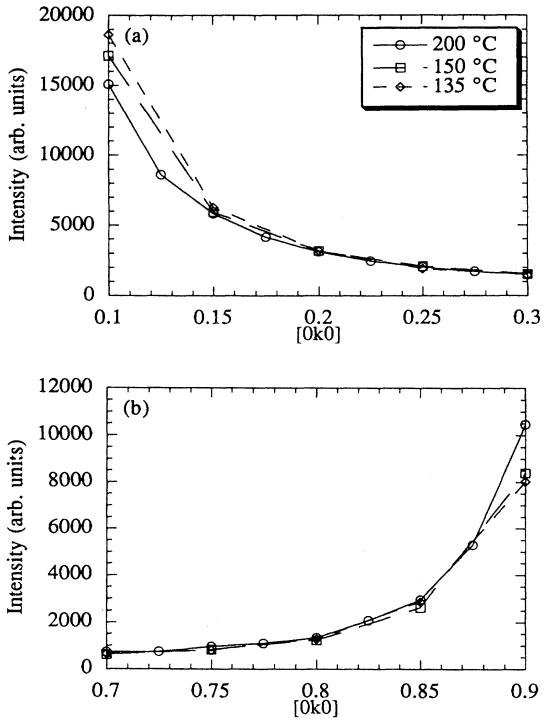

FIG. 4. Temperature dependences of the diffuse scattering intensities around (a) the 400 and (b) the 410 zone centers. Intensity profiles at 200, 150, and 135 °C are taken from the contour maps of Fig. 1(a), (b), and (c) along the [010] ridge for $l=0$ at $h=4.0$.

$k<0.25$. In the previous neutron experiment,[9] the neutron-scattering intensities from the overdamped TO mode also showed a positive temperature dependence in a few Brillouin zones. This positive temperature dependence is possible if the contribution from the $[010]_{TA}$ mode to the TDS intensities for $k>0.75$ is larger than that from the overdamped $[010]_{TO}$ mode. This is so because the $[010]_{TA}$ mode frequencies are relatively temperature independent and the x-ray TDS intensity predicts a lower intensity at lower temperature.[18] In the previous section it was concluded that the static structure factor for the 410 reflection is much smaller than the one for the 400 reflection. It can also be shown that the dynamical structure factor, which is a measure of the diffuse scattering intensities from the optic modes, has the same characteristic behavior. Therefore, the opposite temperature dependence of the x-ray TDS intensities in different zones can be understood.

The current results are consistent with the characteristics of the previous neutron inelastic-scattering results. Especially, the intensity distribution from the overdamped TO mode was well reproduced, as well as the existence of the 2D diffuse scattering pattern. Its temperature dependence is reasonably understood. The current study thus supports Hüller's model. The overdamped TO modes with the ⟨100⟩ polarization may have profound effect on the subsequent ferroelectric phase transformation. On the other hand, the low-frequency relaxational contribution which was observed in Raman-scattering experiments[15] has no measurable effect on the x-ray TDS intensities. Details will be described in a later paper.

The present study was supported by the US Department of Energy via Materials Research Laboratory in University of Illinois at Urbana-Champaign under the Contract No. DEFG02-91ER45439. The experiment was made by using the synchrotron-radiation source at MATRIX beam line X-18A at NSLS at Brookhaven National Laboratory. Laboratoire de Physique, Universite de Bourgogne is associated with the CNRS (URA 1796).

[1]R. Comes, M. Lambert, and A. Guinier, Acta Crystallogr. A **26**, 244 (1970).
[2]R. Comes, M. Lambert, and A. Guinier, Solid State Commun. **6**, 715 (1968).
[3]J. Harada and G. Honjo, J. Phys. Soc. Jpn. **22**, 45 (1967).
[4]M. Holma, H. Hong, M. Nelson, and H. Chen, in *Applications of Synchrotron Radiation Techniques to Material Science*, edited by D. L. Perry, N. Shinn, R. Stockbauer, K. D'Amico, and L. Terminello, MRS Symposia Proceedings No. 307 (Materials Research Society, Pittsburgh, 1993), p. 293.
[5]A. Hüller, Solid State Commun. **7**, 589 (1969).
[6]A. Hüller, Z. Phys. **220**, 145 (1969).
[7]W. Cochran, Advan. Phys. **9**, 387 (1960).
[8]Y. Yamada, G. Shirane, and A. Linz, Phys. Rev. **177**, 848 (1969).
[9]J. Harada, J. D. Axe, and G. Shirane, Phys. Rev. B **4**, 155 (1971).
[10]A. S. Barker, Phys. Rev. **145**, 391 (1966).
[11]M. Didomenico, S. P. S. Porto, and S. H. Wemple, Phys. Rev. Lett. **19**, 855 (1967).
[12]K. A. Müller, W. Berlinger, and K. W. Blazey, Solid State Commun. **61**, 21 (1987).
[13]H. Vogt, J. A. Sanjurjo, and G. Rossbroich, Phys. Rev. B **26**, 5904 (1982).
[14]J. P. Sokoloff, L. L. Chase, and D. Rytz, Phys. Rev. B **38**, 597 (1988).
[15]K. Laabidi, M. Fontana, and B. Jannot, Ferroelectrics **124**, 201 (1991).
[16]R. E. Cohen and H. Krakauer, Phys. Rev. B **42**, 6416 (1990).
[17]G. A. Smolenskii, N. N. Krainik, and S. N. Popov, Sov. Sci. Rev. **6**, 261 (1985).
[18]B. E. Warren, *X-Ray Diffraction* (Addison-Wesley, Reading, MA, 1969), p. 151.
[19]R. J. Nelmes, R. O. Piltz, W. F. Kuhs, Z. Tun, and R. Restori, Ferroelectrics **108**, 165 (1990).